Characterization of Flame-Generated C_{10} to C_{160} Polycyclic Aromatic Hydrocarbons by Atmospheric-Pressure Chemical Ionization Mass Spectrometry with Liquid Introduction via Heated Nebulizer Interface

Arthur L. Lafleur and Koli Taghizadeh

Center for Environmental Health Sciences, Massachusetts Institute of Technology, Cambridge, Massachusetts, USA

Jack B. Howard

Department of Chemical Engineering, Massachusetts Institute of Technology, Cambridge, Massachusetts, USA

Joseph F. Anacleto* and Michael A. Quilliam

Institute for Marine Biosciences, National Research Council, Halifax, Nova Scotia B3H 3Z1, Canada

Complex mixtures of polycyclic aromatic hydrocarbons (PAHs) generated from fuel-rich combustion of ethylene–naphthalene mixtures in a jet-stirred–plug-flow reactor were chemically characterized by combined mass spectrometric techniques to yield product composition data that cover the molecular mass region from simple PAHs (naphthalene, 128 u) to large molecules comparable in molecular size (1792 u) to nanoparticles of soot. Two techniques based on atmospheric-pressure chemical ionization mass spectrometry (APCI-MS) were investigated: (1) APCI-MS combined with high-performance liquid chromatography through a heated nebulizer interface was found suitable for PAHs up to C_{36} (448 u). (2) For the characterization of larger PAHs beyond C_{36}, direct liquid introduction (DLI) of sample into an atmospheric-pressure chemical ionization mass spectrometer through a heated nebulizer gave protonated molecular ions for PAHs over the m/z 400–2000 range. Although unequivocal elemental composition information is unattainable from the unit-resolution DLI/APCI-MS data, by starting with structural data from identified C_{16} to C_{32} PAHs, and applying PAH molecular growth principles, it was possible to generate PAH molecular maps from the DLI/APCI-MS data from which values for the elemental composition could be derived for all major peaks. *(J Am Soc Mass Spectrom 1996, 7, 276–286)*

Polycyclic aromatic hydrocarbons (PAHs) are known mutagens and animal carcinogens and thus pose a potential threat to human health [1–7]. PAH emissions arise when poor fuel–air mixture within combustion devices results in localized fuel-rich pockets, which provide an ideal environment for carbon-compound growth and lead to the formation of PAHs and soot. These products of incomplete combustion can propagate through the combustor and emerge into the atmosphere where they can affect human health. Prediction of the composition of these PAH discharges by using data obtained from research combustors such as the jet-stirred–plug-flow reactor (JSR–PFR) is of great interest, and the goal of an ongoing program in our laboratories is the chemical and toxicological characterization of PAHs in these discharges, so that their impact on human health can be elucidated [8–11].

Previous work in our laboratory established emission yields, molecular structures, and mutagenic potencies for major PAH species produced during the oxygen-deficient combustion of ethylene in the JSR–PFR [10, 11]. A major limitation of earlier work was the difficulty to characterize PAHs whose molecular masses lie beyond the range (~ 300 u) appropriate

Address reprint requests and correspondence to Dr. Arthur L. Lafleur Center for Environmental Health Sciences, Core Laboratory in Analytical Chemistry, Massachusetts Institute of Technology, 77 Massachusetts Avenue, Room 20C-032; Cambridge, MA 02139.

* Present address: Sciex Corporation, 71 Four Valley Drive, Concord, Ontario, Canada L4K 4V8.

1044-0305/96/$15.00
SSDI 1044-0305(95)00651-6

Received June 5, 1995
Revised September 29, 1995
Accepted September 29, 1995

for detection by gas chromatography–mass spectrometry (GC-MS). Until now, the largest PAH we were able to identify unequivocally in flame samples was ovalene (398 u, $C_{32}H_{14}$), which was accomplished through the use of high-performance liquid chromatography (HPLC), although data obtained here and elsewhere [12–16] indicate that even larger PAHs must be present in flames. Indeed, the total absence in flames of PAHs with molecular mass numbers larger than those of simple PAHs (128–398 u) but smaller than those of nanoparticles of soot (~ 2000 u) would be remarkable.

In this study, we adapted techniques previously developed for the identification of C_{60}–C_{92} fullerenes [17–19] to search for large PAHs in flames: (1) atmospheric-pressure chemical ionization mass spectrometry (APCI-MS) combined with HPLC via the heated nebulizer interface (denoted HPLC/APCI-MS) and (2) direct liquid introduction (DLI) of sample into the APCI-MS, also via heated nebulizer interface (denoted DLI/APCI-MS).

Experimental

Combustion Samples

The jet-stirred–plug-flow combustor was designed to provide well defined combustion conditions and its use is part of an ongoing program aimed at understanding and controlling the combustion chemistry responsible for PAH formation. Fuel-rich combustion in a jet-stirred reactor provides baseline input to a close-coupled plug-flow reactor where continuing molecular weight growth reactions occur under conditions similar to those of PAH formation in premixed flames [16]. The jet-stirred–plug-flow reactor has been described previously [8, 9, 20–22].

For these experiments, the combustor primary fuel, which consisted of ethylene and naphthalene, was injected into the plug-flow region to study PAH growth [8, 9]. The following operating parameters were selected: temperature, 1630 K; fuel equivalence ratio, 2.2; flame residence time, 10–12 ms. Under these conditions, the composition of the flame gas at the collection point was the following: total soot, 9.5×10^{-7} g/cm^3 and total tar (dichloromethane-soluble material), 2.2×10^{-7} g/cm^3. Chemical analysis of the tar gave an estimate for total small PAHs (128–226 u) of 3.5×10^{-8} g/cm^3 and for total large PAHs (> 226 u) of 1.8×10^{-7} g/cm^3 [8, 9].

Samples were collected from the combustor by using an aspirated probe connected to a high-yield sampler that consisted of a fluorocarbon filter cartridge (Balston, Inc., Haverhill, MA) backed by two refrigerated (0 °C) traps, each of which contained 1 L of dichloromethane. The probe and filter were washed with dichloromethane and the washings were combined with the trap contents. The samples then were concentrated to 10–20 mL in a Kuderna–Danish evaporative concentrator and filtered through a 0.2-μm fluorocarbon filter to remove particulates. Total tar values were obtained by evaporation of known volumes of the extract and weighing the residue via a previously developed method [23]. Samples were obtained on two occasions to accommodate analysis requirements. One sample was used for the HPLC/APCI-MS experiments and the other for both the GC-MS and DLI/APCI-MS experiments. The concentrations of selected PAHs were determined and are listed in Table 1. Ratios are given with respect to pyrene, for which reference standards are readily available.

Gas Chromatography–Mass Spectrometry

The GC-MS equipment consisted of a Hewlett-Packard (Rockville, MD) 5890II gas chromatograph connected to a model 5972 mass selective detector. Data acquisition and analysis were accomplished by using HP MS-Chemstation software run on a Vectra 486 PC. The gas chromatography (GC) column was a methyl-(5%)-phenyl fused silica column (HP-5, Hewlett-Packard, Inc.) that had a length of 30 m, an inner diameter of 0.25 mm, and a film thickness of 0.25 μm. Helium carrier gas flow was 1.0 mL/min. The injector temperature was 260 °C and the interface was maintained at 280 °C. Injection volume was 1.0 μL. The temperature program consisted of a linear ramp from 50 to 310 °C at 8 °C/min with a final hold at 310 °C for 16 min. The instrument was scanned from m/z 50 to 400 at a rate of 2 scans/s.

High Performance Liquid Chromatography Combined with Atmospheric Pressure Chemical Ionization Mass Spectrometry

The instrument used for HPLC/APCI-MS analysis consisted of an API-III triple quadrupole mass spectrometer (Sciex, Thornhill, Ontario) equipped with a heated nebulizer interface. The interface was modified as previously reported to permit postcolumn doping of the APCI source gas with water vapor to provide an adequate supply of protonating species (H_3O^+) in the source region [18]. The postcolumn water flow was maintained at 10 μL/min with a motor-driven syringe pump. A Hewlett-Packard 1090M liquid chromatograph equipped with a DR5 ternary solvent delivery system, built-in diode-array detector, and HP7994A data system was used for the HPLC/APCI-MS experiments. The column was a Vydac (Separations Group, Hesperia, CA) mini-bore 201TP52 polymeric C_{18} column 25 cm in length with an inner diameter of 2.1 mm. Injection volume was 2.0 μL and the flow rate was 0.2 mL/min. The mobile phase program consisted of 60% aqueous acetonitrile linearly programmed to 100% acetonitrile over 30 min, holding for 5 min be-

fore being linearly programmed to 100% dichloromethane over 40 min and holding for 25 min, then programmed back to the initial conditions in 10 min. Operating conditions were as follows: nebulizer gas (zero air), 90 psig; auxiliary gas (zero air), 1.0 L/min; curtain gas [ultra high purity (UHP) nitrogen], 0.8 L/min; orifice potential, 60 V; scan steps, 1 u; dwell time, 7 ms. The APCI plasma was sustained by corona discharge from a stainless steel needle maintained at 3.0 μA.

Table 1. C_{10}–C_{32} PAHs from fuel-rich ethylene–naphthalene combustion

			Retention time (min)				
C	H	*m/z*	LC-MS[a]	GC-MS[b]	Identification[c]	Peak	Notes[d]
10	8	128	nd	10.5	Naphthalene	—	std
12	8	152	nd	14.3	2-Ethynylnaphthalene	—	C≡C
			8.1	15.1	Acenaphthylene	—	std
13	10	166	nd	17.0	Fluorene	—	std
14	10	176	9.2	18.2	Ethynyl-acenaphthylene isomer	**14a–d**	C≡C
			9.7	18.3	Ethynyl-acenaphthylene isomer	**14a–d**	C≡C
14	12	178	11.5	19.8	Phenanthrene	**14e**	std
			13.1	19.9	Anthracene	**14f**	std
15	10	190	11.6	21.5	Cyclopenta[*def*]phenanthrene	**15a**	std
16	10	202	14.8	23.3	Fluoranthene	**16a**	std
			14.8	23.6	Acephenanthrylene	**16b**	std
			16.3	24.0	Pyrene	**16c**	std
18	10	226	19.4	27.0	Cyclopent[*hi*]acephenanthrylene	**18a**	std
			20.6	26.9	Benzo[*ghi*]fluoranthene	**18b**	std
			20.6	27.6	Cyclopenta[*cd*]pyrene	**18c**	std
20	10	250	24.6	29.7	(Dicyclopenta-pyrene isomer)	**20a–c**	iso.
			26.0	30.5	(Dicyclopenta-pyrene isomer)	**20a–c**	iso.
			27.9	30.8	(Dicyclopenta-pyrene isomer)	**20a–c**	iso.
20	12	252	26.2	31.1	Benzo[*e*]pyrene	**20d**	std
			32.3	31.3	Benzo[*a*]pyrene	**20e**	std
21	12	264	31.3	32.5	(11*H*-Benzo[*def*]cyclopenta[*jkl*]triphenylene)	**21a**	uv, CH_2
			36.4	32.7	(4*H*-Benzo[*def*]cyclopenta[*mno*]chrysene)	**21b**	uv, CH_2
22	12	276	37.0	34.4	Benzo[*ghi*]perylene	**22a**	std
			40.0	34.7	Indeno[1,2,3-*cd*]pyrene	**22b**	std
			46.4	33.4	Anthanthrene	**22c**	std
23	12	288	41.1	35.7	(C_{22} PAH with CH_2 in bay region)	**23a**	iso, CH_2
24	12	300	46.7	37.6	(Coronene isomer)	**24a, b**	iso.
			47.4	37.8	(Coronene isomer)	**24a, b**	iso.
			48.8	38.5	Coronene	**24c**	std
25	12	312	48.5	41.0	($C_{23}H_{12}$ with added cyclopenta group)	**25a**	iso, CH_2
26	12	324	53.5	42.4	($C_{22}H_{12}$ PAH with 2 cyclopenta-fused rings)	**26a, b**	iso.
			54.3	44.8	($C_{22}H_{12}$ PAH with 2 cyclopenta-fused rings)	**26a, b**	iso.
			55.5	45.3	(Cyclopenta[*bc*]coronene)	**26c**	iso.
28	12	348	61.6	nd	(Dicyclopenta-coronene isomer)	**28a, b**	iso.
			62.0	nd	(Dicyclopenta-coronene isomer)	**28a, b**	iso.
28	14	350	63.6	nd	Benzo[*pqr*]naphtho[8,1,2-*bcd*]perylene	**28c**	uv
			68.3	nd	(Unknown)	—	iso
30	14	374	73.2	nd	Naphtho[8,1,2-*abc*]coronene	**30a**	std
32	14	398	80.0	nd	Ovalene	**32a**	std

[a] LC-MS: High-performance liquid chromatography with atmospheric-pressure chemical ionization mass spectrometry via heated nebulizer interface.
[b] GC-MS: Gas chromatography with electron-impact mass spectrometry; nd = not detected.
[c] Listed in parentheses are provisionally assigned structures that lack confirmation with standards.
[d] std denotes structure confirmed by using reference standard; C≡C denotes terminal triple bond determined by using GC–Fourier transform infrared spectrometry; CH_2 denotes the presence of methylene group suggested by prominent [M - 1] peak in GC-MS; uv denotes that the UV spectrum supports assigned structure; iso. denotes specific iosmer(s) unknown, tentative identification only.

Direct Liquid Introduction–Atmospheric Pressure Chemical Ionization Mass Spectrometry

The mass spectrometer used for DLI/APCI-MS analysis was an API-I single-quadrupole mass spectrometer (Sciex) equipped with a heated nebulizer interface. The instrument was controlled with Sciex API operating software run on a Macintosh Quadra 950 computer (Apple Computer, Cupertino, CA). The direct liquid injection system consisted of a Beckman Instruments (Fullerton, CA) model 126 pumping system coupled directly to the heated nebulizer via a Rheodyne (Cotati, CA) bypass-type injector with a 20-μL loop. The pumping system was controlled via Beckman System Gold software run on an IBM PS/2 486DX2/66 computer (IBM, Boca Raton, FL). Dichloromethane was used as the mobile phase. The flow rate was 0.4 mL/min and the nebulizer heater was set at 480 °C, a condition where sample and nebulizer gas would experience a temperature of 85–95 °C.

To obtain a mass spectrum that covers a wide mass range (400–2200 u) in a dynamic system with a small sample size, the mass spectrum was divided into overlapping regions of m/z 200–220 units each and these were later combined into one spectrum by using the appropriate computer software. Operating conditions were as follows: nebulizer gas (UHP zero air) pressure, 80 psig; auxiliary gas (UHP zero air) 1.0 L/min; curtain gas (UHP nitrogen), 0.8 L/min; orifice potential, 80 V; interface temperature, 60 °C; scan steps, 1 u; dwell time, 3–4 ms. The APCI plasma was sustained by a corona discharge from a stainless steel needle maintained at 3.0 μA.

Chemicals and Reference Materials

Dichloromethane, acetonitrile, and methanol were Caledon glass-distilled solvents obtained from American Bioanalytical (Natick, MA). A standard reference mixture of PAHs was obtained from the U.S. National Institute for Standards and Technology (SRM 1647) and included the following 16 PAHs: naphthalene, acenaphthylene, acenaphthene, fluorene, anthracene, phenanthrene, fluoranthene, pyrene, chrysene, benz[*a*]anthracene, benzo[*b*]fluoranthene, benzo[*k*]-fluoranthene, benzo[*a*]pyrene, indeno[1,2,3-*cd*]pyrene, dibenz[*a,h*]anthracene, and benzo[*ghi*]perylene. Reference quantities of cyclopenta[*cd*]pyrene, cyclopent[*hi*]aceanthrylene, and cyclopent[*hi*]acephenanthrylene were synthesized by J. Lugtenburg and J. Cornelisse. Samples of naphtho[8,1,2-*abc*]coronene, ovalene, and benzo[*pqr*]naphtho[8,1,2-*bcd*]perylene were furnished by J. Fetzer.

Safety note. Many of the PAHs mentioned in this study are mutagenic in human cells and tumorigenic in animal tests. Cyclopenta[*cd*]pyrene and benzo[*a*]-pyrene are especially potent mutagens and tumorigens [4–7]. All PAHs should be considered potentially harmful to humans and should be handled accordingly.

Results and Discussion

A number of fuel-rich ethylene–naphthalene combustion samples were generated under controlled conditions and prepared for analysis as detailed in the Experimental section. Because GC-MS is used often and is widely accepted as one of the most powerful methods for PAH analysis, we used it as the benchmark for comparison with the other methods studied here [1, 2, 10]. The GC-MS total ion chromatogram is shown in Figure 1. The mass spectral data indicate a PAH size distribution ranging from 152 (acenaphthylene) to 324 u. In GC-MS, detection is governed strongly by volatility and thus GC elution potential. For the GC-MS system used in this study, the molecular mass limit for PAH detection approximates 324 u for planar PAHs and at least 354 u for biarenes such as bianthracene [24]. The detection of PAHs up to 402 u by using a GC-MS instrument optimized for the detection of large PAHs has been reported [25]. Identification of the numbered components is found in Table 1.

The PAH size limitation imposed by the gas chromatograph can, in principle, be overcome by replacing the GC separation step with a step based on HPLC. However, in practice, mass spectrometers suitable for GC detection generally prove inadequate for use with HPLC because of the large differences in operating environment between the two techniques. A specialized liquid chromatography–mass spectrometry (LC-MS) instrument usually is employed and Figure 2 shows a LC-MS total ion chromatogram obtained from

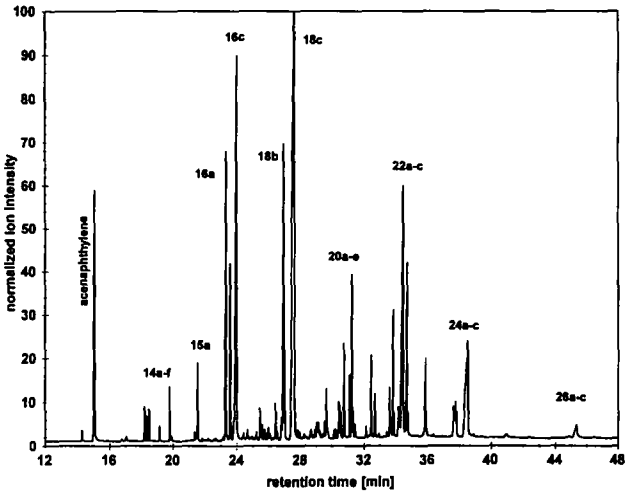

Figure 1. GC-MS total ion chromatogram of a fuel-rich ethylene–naphthalene combustion sample from a jet-stirred–plug-flow reactor. Data for numbered peaks are found in Table 1. Molecular structures of components are shown in Figures 3a and 3b.

such an instrument. The instrument used here consists of a high-performance liquid chromatograph coupled with an atmospheric-pressure chemical ionization mass spectrometer via a heated nebulizer interface [17–19]. Again, the designated peaks refer to data in Table 1. The three-digit numbers below the chromatogram baseline are molecular mass values recorded for the PAHs in the peaks above the baseline. The APCI technique used here generates protonated molecular ions [M + 1] for PAHs. The mass values given for the PAHs indicated take this into account. In both chromatograms, the numbers above the peaks refer to molecular structures illustrated in Figures 3a and 3b.

There are some significant differences between the data generated by the two techniques. First, GC-MS, but not HPLC/APCI-MS, is able to detect a number of volatile components, which include phenylacetylene and indene, that are not listed in Table 1. Second, HPLC/APCI-MS is able to detect PAHs with molecular mass beyond the range accessible with GC-MS. Large PAHs (> 226 u) are clearly more abundant in the LC-MS chromatogram (Figure 2) and the mass range for PAHs is extended to 448 u. For example, the PAH cluster at 324 u, barely detectable in the GC-MS data, is much more pronounced in the LC-MS data and can be seen to include at least three isomers. The composition of the flame sample has been determined for fixed gases, hydrocarbons, and PAHs [8–10]. Data for selected PAHs are found in Table 2. The different PAH concentrations and amounts injected reflect differences in concentration factor and injection volume for the methods involved, although the PAH distribution remains the same. The PAH distribution profile in the HPLC/APCI-MS chromatogram more closely reflects the sample composition in Table 2 than does the GC-MS chromatogram, principally because a significant fraction of the PAHs in this sample are not amenable to gas chromatography for reasons discussed earlier.

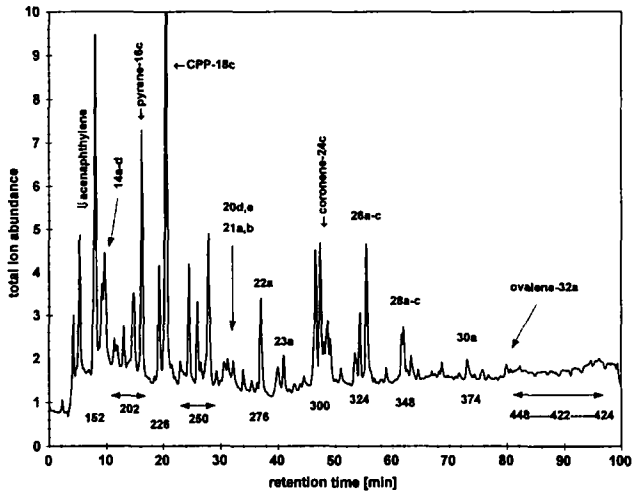

Figure 2. LC-MS total ion chromatogram of a fuel-rich ethylene–naphthalene combustion sample from a jet-stirred–plug-flow reactor. Data obtained by using high-performance liquid chromatography (Vydac 201TP52 column) coupled with atmospheric-pressure chemical ionization mass spectrometry via heated nebulizer interface (HPLC/APCI-MS). Peak data are found in Table 1 and structures of designated components are shown in Figures 3a and 3b. The three-digit numbers (152–448) below selected peak clusters represent the predominant mass-to-charge ratio values observed for each cluster.

Not obvious from the GC-MS and HPLC/APCI-MS data are differences in the types of mass spectra obtained from the two techniques. Atmospheric-pressure chemical ionization is a soft ionization method [26] and gives protonated molecular ions for PAHs with no discernible fragmentation. Electron-impact (EI) mass spectrometry is more energetic in nature [26], but the stability of the PAH radical ions produced upon electron impact also results in little or no fragmentation for PAHs [2]. Mass spectra therefore are not generally useful in structural elucidation of isomeric PAHs [2]. However, when a PAH incorporates certain substituents or structural features, characteristic fragments can appear in its EI mass spectrum. We used this observation to identify PAHs with cyclopenta-fused rings formed by methylene ($-CH_2-$) insertion into a bay region. Examples are **15a**, **21a**, and **21b**, in Figure 3a and **25a** and **25b**, in Figure 3b. The EI mass spectrum in these species exhibits a characteristic feature of an abundant $[M - 1]^+$ ion that approximates the molecular ion $[M]^+$ in intensity.

In spite of the differences observed between the two techniques, it is remarkable how similar the PAH distribution patterns are for the two methods when it is considered how different the source environments are between GC-MS and HPLC/APCI-MS. The GC-MS has an evacuated ion source and generates ions by electron bombardment, whereas the HPLC/APCI-MS source operates at atmospheric pressure and relies primarily on chemical ionization to produce ions. Also, in the HPLC/APCI-MS experiments, the gaseous environment of the ion source varies in step with programmed shifts in the HPLC mobile phase composition.

The HPLC/APCI-MS data allows some additional conclusions to be made with regard to the structural class of some of the unknown PAHs by consideration of HPLC retention behavior. In the m/z 300 cluster, for example, the peak that corresponds to coronene is one of the later to elute in this group. Other work has demonstrated that elution of PAH isomers on this type of column (Vydac 201TP, polymeric C18) proceeds according to increasing length-to-breadth ratio (L/B) for planar PAHs and according to degree of planarity for nonplanar PAHs [27, 28]. The L/B ratio for the highly symmetrical coronene is 1.0; therefore, the LC-MS data strongly suggest that the earlier eluting 300-u PAH isomers must be nonplanar—a condition that could be fulfilled by the presence of an externally

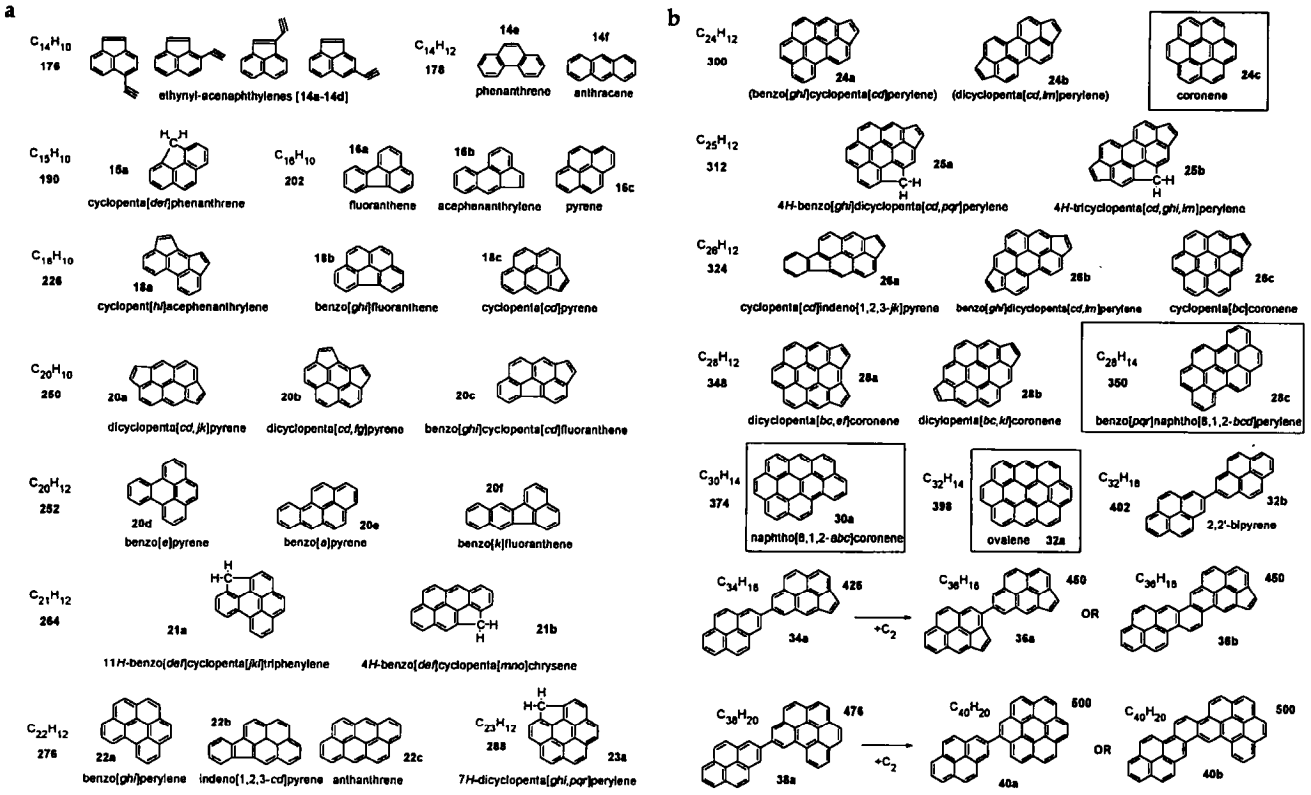

Figure 3. (a) Molecular structures of C_{14}–C_{23} polycyclic aromatic hydrocarbons found in ethylene–naphthalene flame samples. (b) Suggested molecular structures of C_{24}–C_{40} polycyclic aromatic hydrocarbons found in ethylene–naphthalene flame samples. The identities of outlined structures were confirmed with reference standards.

fused cyclopenta group. Examples of such structures are **24a** and **24b** in Figure 3b. We also have observed that PAHs above 400 u do not consistently elute in order of increasing molecular mass. This result agrees with predictions from HPLC studies on larger PAHs where isomers with varying molecular topology are increasingly abundant and shape effects become the governing factor in PAH elution [27, 28].

Atmospheric Pressure Chemical Ionization–Mass Spectrometry with Direct Liquid Introduction

The HPLC/APCI-MS results suggest that, via existing column technology, an upper limit for the HPLC analysis of PAHs is reached at about 450 u. First of all, the structural complexity and large number of possible isomers of PAH in this mass range make it difficult to

Table 2. Sample composition for selected PAH

	Sample component	Structure reference[a]	Molecular weight	Relative amount[b]	Amount injected		
					GC-MS	HPLC/APCI-MS	DLI/APCI-MS
1	Pyrene	**16c**	202	1.0	120 ± 12 ng	43 ± 4 ng	430 ± 40 ng
2	Cyclopenta[*cd*]pyrene	**18c**	226	1.8	210 ± 18 ng	79 ± 6 ng	790 ± 60 ng
3	Benzo[*ghi*]perylene	**22a**	276	0.36	43 ± 12 ng	16 ± 4 ng	160 ± 40 ng
4	Coronene	**24c**	300	0.39	45 ± 9 ng	17 ± 3 ng	170 ± 30 ng
5	Cyclopenta[*bc*]coronene	**26c**	324	0.81	94 ± 25 ng	35 ± 9 ng	350 ± 90 ng
6	Naphtho[8,1,2-*abc*]coronene	**30a**	374	0.22	26 ± 9 ng	9.6 ± 3 ng	96 ± 30 ng
7	Total amount injected	—	—	—	3.2 ± 0.3 μg	1.2 ± 0.1 μg	12 ± 1 μg
8	Σ[PAH > 226][c]	—	—	—	2.6 ± 0.3 μg	0.98 ± 0.1 μg	9.8 ± 1 μg

[a] Refers to structures illustrated in Figures 3a and 3b and data listed in Table 1.
[b] Values listed are relative amounts based on pyrene = 1.0.
[c] Calculated value for total mass of PAH > 226 u in the sample [8].

predict HPLC retention behavior. This problem has been studied elsewhere by using large PAH model compounds [29–31]. Second, it appears that the elution of PAHs larger than 450 u may be inefficient with these columns, and other methods must be used to introduce the sample into the mass spectrometer. To this end, we dispensed with the HPLC column and introduced the sample by direct liquid injection (DLI) into the ion source of the APCI-MS.

Figure 4 shows the mass spectrum of an ethylene–naphthalene flame sample obtained by direct liquid injection into an atmospheric-pressure chemical ionization mass spectrometer via heated nebulizer interface (DLI/APCI-MS). Ion abundances were normalized to m/z 599. Because APCI is a soft ionization method and because ion formation is governed by protonation by H_3O^+, all peaks are assumed to be protonated PAH parent ions $[M + 1]^+$, in contrast to electron-bombardment methods (e.g., in GC-MS), where the parent ions are all even-mass M^+ ions. At lower carbon numbers ($< C_{100}$), the most abundant parent ions are odd-numbered, but at higher carbon numbers ($> C_{100}$) the contribution from isotopic ^{13}C leads to the dominance of even-numbered protonated molecular ions. Because

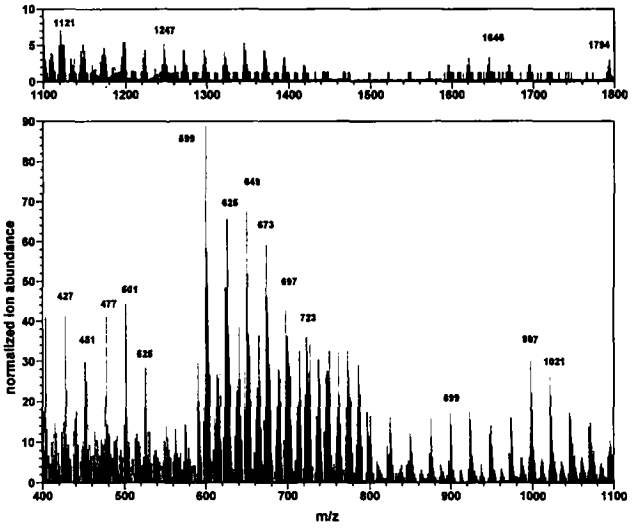

Figure 4. High-range mass spectrum of ethylene–naphthalene flame sample obtained by direct liquid injection of sample into an atmospheric-pressure chemical ionization mass spectrometer via heated nebulizer interface (DLI/APCI-MS). Ion abundances were normalized to that of m/z 599. Ion formation for PAHs depends on protonation by H_3O^+ so PAH molecular ions are $[M + 1]$ ions.

Table 3. DLI/APCI-MS data for fuel-rich ethylene–naphthalene flame sample

Rank[a]	Mass[b]	Intensity[c]	Rank	Mass	Intensity	Rank	Mass	Intensity
1	598	100.0	26	474	24.0	51	404	14.7
2	648	75.9	27	526	20.6	52	562	14.7
3	624	73.6	28	440	19.6	53	436	14.4
4	672	66.6	29	922	19.5	54	462	14.2
5	622	54.2	30	400	19.4	55	530	14.0
6	500	49.5	31	796	19.4	56	422	14.0
7	696	48.0	32	1044	19.2	57	528	14.0
8	426	46.4	33	898	19.2	58	576	13.9
9	476	46.4	34	800	18.2	59	744	13.8
10	402	45.7	35	454	18.0	60	416	13.6
11	722	40.2	36	824	18.0	61	848	13.6
12	726	38.5	37	874	17.9	62	480	13.5
13	772	36.5	38	972	17.8	63	412	13.5
14	750	36.3	39	610	17.7	64	514	13.4
15	996	33.6	40	438	17.5	65	946	13.4
16	450	33.3	41	670	17.2	66	490	13.0
17	524	31.8	42	414	16.9	67	634	12.8
18	646	30.7	43	424	16.7	68	850	12.4
19	748	30.7	44	1070	16.4	69	552	12.4
20	612	29.9	45	574	16.0	70	620	12.4
21	1020	29.4	46	478	15.9	71	512	12.2
22	452	27.9	47	498	15.8	72	464	11.9
23	428	25.6	48	550	15.8	73	466	11.8
24	596	25.4	49	948	15.6	74	470	11.8
25	720	24.2	50	1068	15.2	75	1094	11.8

[a] Rank based solely on DLI/APCI-MS data, not relative to total PAHs.
[b] Mass (u) of PAH: assumes [M + 1] molecular ions in APCI-MS data.
[c] Relative intensity: intensity of m/z 599 peak ([M + 1] ion of 598-u PAH) = 100.

of the stability of the PAH parent ions to fragmentation and because APCI is a soft ionization method, PAH fragment ions are practically nonexistent. The 75 most abundant peaks are listed in Table 3 in order of decreasing relative abundance. The observed $[M + 1]^+$ ions are converted to PAH molecular mass values. In the mass spectrum shown in Figure 4, over 150 peaks with relative abundance greater than 2.0% of the base peak could be discerned.

The DLI/APCI-MS instrument affords mass spectra (to m/z 2000) with unit resolution, a degree of performance not good enough for us to derive, a priori, the elemental composition of each ion. However, by starting with the molecular structures of the most abundant and highly characterized C_{16}–C_{32} PAHs and applying PAH molecular-weight growth principles, it is possible to convert the DLI/APCI-MS data into PAH molecular maps from which values could be derived for the elemental composition of all major peaks.

First of all, combination of the GC-MS and LC-MS data illustrated in Figures 1 and 2, respectively, with other data obtained in our laboratories enabled PAH molecular growth to be traced from small hydrocarbons, (e.g., acetylene, C_2), to much larger PAHs (e.g., ovalene, C_{32}) for the particular combustor and operating conditions used in this work. PAH molecular growth research is a worldwide ongoing enterprise and cannot be summarized in one diagram. However, the information that is needed to interpret the bulk of our mass spectral data can be derived in this way. A diagram derived from the GC-MS and LC-MS data for PAHs ($> C_{12}$) and also from previously published data for aromatics and acetylenes (C_2–C_{12}) is illustrated in Figure 5. The numbers in boxes indicate PAH molecular mass values. Ordinate values of 2–32 give the number of carbon atoms for PAHs and their precursors and the number of hydrogens from 2 to 14 are plotted along the abscissa. In terms of PAH molecular growth, descent vertically in a row is the equivalent of the addition of one carbon atom; two rows equals two carbons. Molecular growth of C_4H_2 is illustrated by the arrows that connect selected PAH molecular mass values that differ by 50 u.

It should be noted that flame-generated PAH mixtures can be very complex and many other PAHs are formed in the JSR/PFR. However, only the predominant species were included in Figure 5. Although only one box is used for each C/H value, many isomeric PAHs that have the same C/H composition are possible; the number of isomers generally increases with molecular mass. For example, as shown in Table 1, at least 3 PAHs that have an elemental composition of $C_{16}H_{10}$ have been identified. Fortunately, several important factors act in consort to limit the complexity of the PAH product distribution from our combustion samples. First of all, the number of theoretically stable PAH structures is limited at the high temperature (1600 K) used in our experiments [34]. Second, the

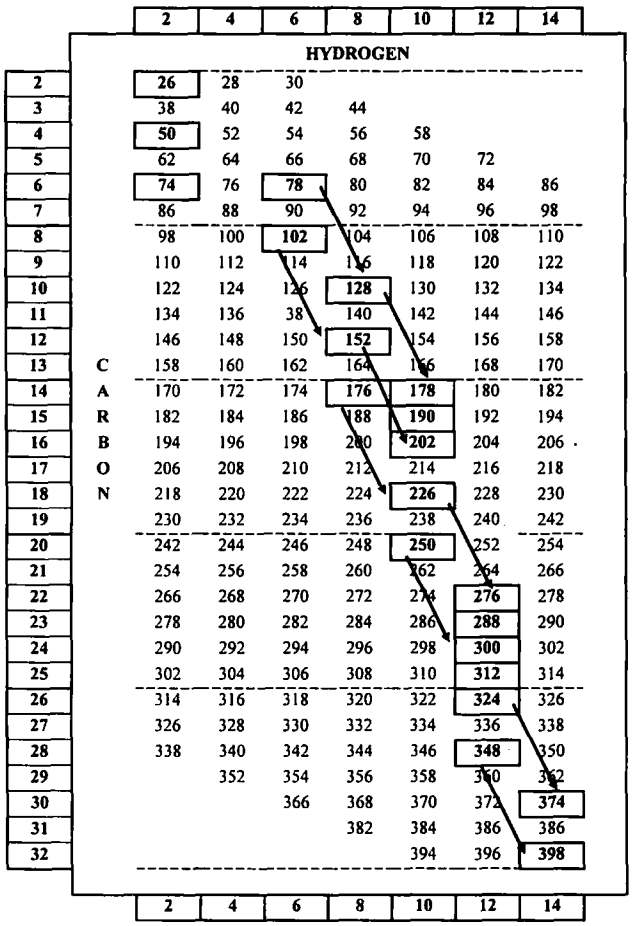

Figure 5. PAH molecular growth from acetylene (C_2) to ovalene (C_{32}). The diagram was constructed by using data from several sources, which include the GC-MS and HPLC/APCI-MS experiments and earlier work [8, 10, 11].

complete mixture of fuel and oxidant before combustion prevents the formation of oxidant-depleted pockets or thermally deficient zones that could lead to alternative product distributions. It is also important that the combination of fuel-rich conditions, high temperatures, and well-mixed reactants ensure the paucity of oxygenated PAHs, a condition that simplies the interpretation of the data [8, 10, 20].

Referring to Figure 5, it is seen that starting from benzene at 78 u, larger molecules are formed principally by C_2 addition (e.g., addition of acetylene to phenyl radical followed by hydrogen elimination) to yield phenylacetylene at 102 u (78 u + 24 u). Addition of another acetylene to an ortho radical site on phenylacetylene followed by hydrogen addition and cyclization yields naphthalene at 128 u (78 u + 50 u). Alternatively, a C_4 addition [e.g., addition of C_4H_2 (diacetylene) to phenyl radical] also can lead to naphthalene.

Benzene itself can be formed from simple hydrocarbons in a number of ways: The combination of an acetylene molecule with a C_4H_5 radical is thought to

occur in one pathway, whereas another pathway involves the combination of two C_3 hydrocarbon radicals. The hydrocarbons C_3H_4 and C_4H_6 have been detected in the JSR/PFR flames, and C_3H_3 and C_4H_5 undoubtedly are present based on the radical detection methods used in similar systems [16], but their role in PAH formation is beyond the scope of this work. The cited C_2 (+24 u) and C_4 (+50 u) radical addition reactions, represented here solely by the overall molecular steps, undoubtedly are more complex than shown in Figure 5, where they are reduced to simple molecular mass increases. However, this simple process is sufficient to describe the formation of the predominant PAHs detected in flames. Other PAHs of lower abundance can be formed by C_1 addition (e.g., insertion of methylene in the PAH bay region followed by hydrogen elimination). An example is the formation of cyclopenta[*def*]phenanthrene (190 u) from phenanthrene (178 u). Certain PAHs of 264, 288, and 312 u also are known to contain a bay-region methylene group.

Based on these simple PAH molecular-weight growth principles, the DLI/APCI-MS data can be converted to a molecular map, shown in Figure 6, from which we may deduce elemental composition. This map was constructed by using principles illustrated in the PAH molecular growth diagram depicted in Figure 5. As in Figure 5, the boxed numbers in Figure 6 refer to molecular mass values for abundant PAHs, now derived solely from the mass spectrometry data shown in Figure 4. PAH carbon number is plotted on the abscissa and hydrogen number is plotted on the ordinate. Figure 6 includes data for C_{32}–C_{144} PAHs and starts with a PAH of 398 u, the most abundant isomer of which is ovalene, $C_{32}H_{14}$ (**32a** in Figure 3b),

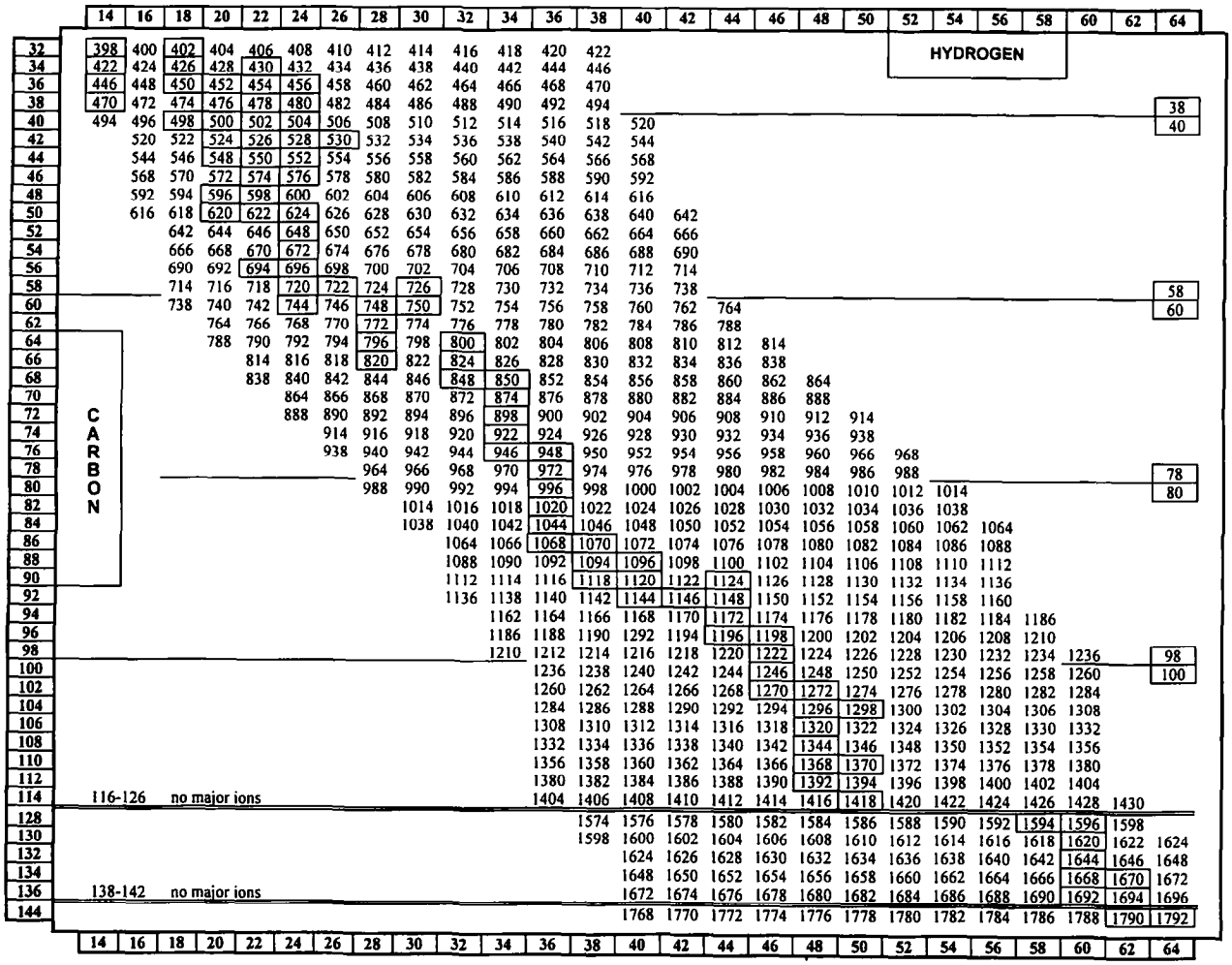

Figure 6. DLI/APCI-MS data for C_{32}–C_{144} polycyclic aromatic hydrocarbons converted to a molecular map. The abscissa values represent the number of carbon atoms from 32 to 144, whereas the ordinate values from 14 to 64 refer to the number of hydrogens. The three- and four-digit numbers in the chart represent molecular mass values calculated for selected combinations of C and H. Numbers enclosed in rectangular borders correspond to PAH molecular mass values for which a significant peak (> 2% total ion abundance) was observed in the DLI/APCI-MS experiments. The C_{116}–C_{126} and C_{138}–C_{142} ranges were omitted due to scarcity of significant ions. Odd-carbon number data were omitted for clarity.

which is formed by C_2 addition to $C_{30}H_{14}$ (e.g., naphtho[8,1,2-*abc*]coronene, **30a** in Figure 3b).

Another possible composition for a PAH of 398 u might be $C_{31}H_{26}$; however, this species could not be formed from a smaller PAH by known addition routes (C_1, C_2, or C_4H_2) and also, its C/H ratio precludes it from being totally aromatic. Other species of 398 u that have an additional carbon atom ($C_{33}H_2$) are possible also but would have too few hydrogens to be PAHs. Therefore, $C_{32}H_{14}$ is the only plausible molecular formula for a PAH of 398 u. The reasons detailed in the preceding text for the absence of plausible structures for C_{31} and C_{33} PAHs of 398 u help to explain the relatively low abundance observed for odd-carbon PAHs. As we saw earlier, the predominant route to odd-carbon flame-generated PAHs is through methylene insertion (C_1 addition) into a PAH bay region, and this fact limits the number of PAHs that can accommodate such an insertion. High flame temperatures (> 1500 K) favor the conversion of PAHs with methyl or other alkyl substituents to unsubstituted species [35, 36], so their abundance is very low in our flames. The C_3 hydrocarbons, whose addition (e.g., as C_3H_3 radical) to even-carbon species could give odd-carbon PAHs, do not appear to be present in large enough concentration in the later stages of PAH growth to be a significant reactant in odd-carbon PAH formation. In Figure 6, odd-carbon PAHs are omitted because of their relatively low abundance. For C_{34}–C_{144} PAHs, possible structures must be derived with some degree of speculation because of the paucity of data for PAHs this large.

Practical and reliable instrumentation for the analysis of selected PAHs by LC-MS has become available recently and some results in this area have begun to appear [37, 38]. The study of large PAHs also has begun in earnest [12, 13] and the utilization of LC-MS techniques for the characterization of these species has only begun. Nevertheless, it appears highly likely that the HPLC/APCI-MS and DLI/APCI-MS methods described here will be applicable to the analysis of PAHs from many different sources. However, complexity of the sample remains a major limitation to the usefulness of these techniques until better separation techniques for large PAHs become available. Although PAHs with fewer than eight to nine fused rings were separated with acceptable efficiency, the separation of larger PAHs still poses a challenge.

The development of novel separation methods for larger PAHs is likely to have a great impact on the degree to which DLI/APCI-MS can be applied to the study of more complex mixtures of large PAHs associated with fossil fuels and their combustion products. The great complexity of fossil fuel products is well known and their chromatographic separation has been studied for decades [39, 40]. Fossil fuel combustion samples from commercial equipment often contain unburned or partially oxidized fuel components in addition to pyrosynthesized PAHs, and these mixtures can be too complex for direct analysis by low-resolution, single-stage mass spectrometers. At present, DLI/APCI-MS shows the greatest promise in the analysis of complex mixtures of PAHs generated from laboratory combustors or commercial combustors that burn simple fuels such as natural gas. To our knowledge, the C_{144} PAHs at 1790 and 1792 u are the largest flame-generated PAHs ever detected and are comparable in size to nanoparticles of soot. Future work with this method surely will shed additional light on the production of soot, PAHs and other carbonaceous species in flames.

Acknowledgment

This investigation was supported in part by the National Institute of Environmental Health Sciences Center (Grant NIH-5P30-ESO2109) and the Health Effects of Fossil Fuels Utilization Program (Grant NIH-5P01-ESO1640). The DLI/APCI-MS work was supported by an instrumentation grant (DE-FG05-92ER7811) provided by the U.S. Department of Energy. We thank John Fetzer of Chevron Research and J. Cornelisse and J. Lugtenburg of Leiden University for providing us with reference quantities of PAH standards. We thank Joseph A. Marr for assisting in the collection of the flame samples.

References

1. Grimmer, G., Ed. *Environmental Carcinogens: Polycyclic Aromatic Hydrocarbons;* CRC Press: Boca Raton, FL, 1983.
2. Lee, M. L.; Novotny, M. V.; Bartle, K. D. *Analytical Chemistry of Polycyclic Aromatic Compounds;* Academic Press: New York, 1981.
3. Prado, G.; Westmoreland, P. R.; Andon, B. H.; Leary, J. A.; Biemann, K.; Thilly, W. G.; Longwell, J. P.; Howard, J. B. In *Chemical Analysis and Biological Fate: Polynuclear Aromatic Hydrocarbons. Proceedings, Fifth International Symposium on Polynuclear Aromatic Hydrocarbons;* Cooke, M.; Dennis, A. J., Eds.; Battelle: Columbus, Ohio, 1981, pp 189–198.
4. Kaden, D. A.; Hites, R. A.; Thilly, W. G. *Cancer Res.* **1979,** *39,* 4152–4159.
5. Fu, P. P.; Beland, F. A.; Yang, S. K. *Carcinogenesis* **1980,** *1,* 725–727.
6. Busby, W. F.; Stevens, E. K.; Kellenbach, E. R.; Cornelisse, J.; Lugtenburg, J. *Carcinogenesis* **1988,** *9,* 741–746.
7. Busby, W. F.; Goldman, M. E.; Newberne, P. M.; Wogan, G. N. *Carcinogenesis* **1984,** *5,* 1311–1316.
8. Marr, J. A. Ph.D. Thesis, Massachusetts Institute of Technology, 1993.
9. Marr, J. A.; Giovane, L. M.; Longwell, J. P.; Howard, J. B.; Lafleur, A. L. *Combust. Sci. Technol.,* **1994,** *101,* 301–304.
10. Lafleur, A. L.; Longwell, J. P.; Monchamp, P. A.; Shirname-More, L.; Peters, W. A.; Plummer, E. F. *Energy Fuels* **1990,** *4,* 307–319.
11. Lafleur, A. L.; Longwell, J. P.; Marr, J. A.; Monchamp, P. A.; Plummer, E. F.; Thilly, W. G.; Mulder, P. P. Y.; Boere, B. B.; Cornelisse, J.; Lugtenburg, J. *Environ. Health Perspec.* **1993,** *101,* 146–153.
12. Fetzer, J. C.; Biggs, W. R. *Polycyclic Aromatic Compounds* **1994,** *4,* 3–17.
13. Fetzer, J. C.; Biggs, W. R. *Polycyclic Aromatic Compounds* **1994,** *5,* 193–199.

14. Peaden, P. A.; Lee, M. L.; Hirata, Y.; Novotny, M. *Anal. Chem.* **1980,** *52,* 2268–2271.
15. Smedley, J. M.; Williams, A.; Bartle, K. D. *Polycyclic Aromatic Compounds* **1994,** *4,* 61–70.
16. Bittner, J. D.; Howard, J. B. *Particulate Carbon: Formation During Combustion;* Plenum Press: New York, 1981; pp 109–142.
17. Anacleto, J. F.; Quilliam, M. A.; Boyd, R. K.; Howard, J. B.; Lafleur, A. L.; Yadav, T. *Rapid Commun. Mass Spectrom.* **1993,** *7,* 229–234.
18. Anacleto, J. F.; Boyd, R. K.; Pleasance, S.; Quilliam, M. A.; Howard, J. B.; Lafleur, A. L.; Makarovský, Y. *Can. J. Chem.* **1992,** *70,* 2558–2568.
19. Anacleto, J. F.; Perreault, H.; Boyd, R. K.; Pleasance, S.; Quilliam, M. A.; Sim, G. P; Howard, J. B.; Makarovsky, Y.; Lafleur, A. L. *Rapid Commun. Mass Spectrom.* **1992,** *6,* 214–220.
20. Nenniger, J. E.; Kridiotis, A.; Chomiak, J.; Longwell, J. P.; Sarofim, A. F. *20th International Symposium On Combustion;* The Combustion Institute, 1985, pp 473–479.
21. Lam, F. W.; Howard, J. B.; Longwell, J. P. *22nd International Symposium on Combustion;* The Combustion Institute, 1989, pp 323–332.
22. Vaughn, C. B.; Howard, J. B.; Longwell, J. P. *Combust. Flame* **1991,** *87,* 278–288.
23. Lafleur, A. L.; Monchamp, P. A.; Plummer, E. F.; Kruzel, E. L. *Anal. Lett.* **1986,** *19,* 2103–2119.
24. Wornat, M. J.; Lafleur, A. L.; Sarofim, A. F. *Polycyclic Aromatic Compounds* **1993,** *3,* 149–161.
25. Romanowski, T.; Funcke, W.; König, J.; Balfanz, E. *J. High Res. Chromatogr. Chromatogr. Commun.* **1981,** *4,* 209–214.
26. McLafferty, F. W.; Turecek, F. *Interpretation of Mass Spectra, 4th ed.;* University Science Books: Mill Valley, CA, 1993.
27. Sander, L. C.; Wise, S. A. *J. Chromatogr. A* **1993,** *656,* 335–351.
28. Wise, S. A. In *Handbook of Polycyclic Aromatic Hydrocarbons;* Bjørseth, A.; Ed.; Marcel Dekker: New York, 1983; pp 183–256.
29. Fetzer, J. C.; Rechsteiner, C. E. In *Polynuclear Aromatic Compounds: Measurement Means and Metabolism;* Cooke, M.; Loening, K.; Merritt, J., Eds.; Battelle Press: Columbus, OH, 1991; pp 259–270.
30. Fetzer, J. C.; Biggs, W. R. *J. Chromatogr.* **1984,** *295,* 161–169.
31. Fetzer, J. C.; Biggs, W. R. *J. Chromatogr.* **1985,** *346,* 81–92.
32. Sander, L. C.; Wise, S. A. In *Advances in Chromatography,* vol. 25; Giddings, J. C.; Grushka, E.; Cazes, J.; Brown, P. R., Eds.; Marcel Dekker: New York, 1986; pp 139–218.
33. Standard Reference Data Program, *NIST / NIH / EPA Mass Spectral Library;* National Institute of Standards and Technology, 1994.
34. Stein, S. E.; Fahr, A. *J. Phys. Chem.* **1985,** *89,* 3714–3725.
35. Wornat, M. J.; Sarofim, A. F.; Longwell, J. P. *Energy Fuels* **1987,** *1,* 431–437.
36. Wornat, M. J. Ph.D. Thesis, Massachusetts Institute of Technology, Cambridge, MA, 1988.
37. Quilliam, M. A.; Sim, P. G. *J. Chromatogr. Sci.* **1988,** *26,* 160–167.
38. Anacleto, J. F.; Ramaley, L.; Benoit, F. M.; Boyd, R. K.; Quilliam, M. A. *Anal. Chem.* **1995,** *67,* 4145–4154.
39. Bartle, K. D.; Collin, G.; Stadelhofer, J. W.; Zander, M. *J. Chem. Tech. Biotechnol.* **1979,** *29,* 531–551.
40. Altgelt, K. H.; Gouw, T. H. *Adv. Chromatogr.* **1975,** *13,* 71–175.